SESSION 15

The Sun: Our own backyard plasma laboratory

Peter R. Young[1,2]

[1]NASA Goddard Space Flight Center, Greenbelt, MD 20771, USA
[2]Northumbria University, Newcastle-Upon-Tyne, UK

Abstract. The Sun's atmosphere increases in temperature from 6000 degrees at the surface to over a million degrees at heights of a few thousand kilometers. This surprising temperature increase is still an active area of scientific study, but is generally thought to be driven by the dynamics of the Sun's magnetic field. The combination of a 2-to-3 order of magnitude temperature range and a low plasma density makes the solar atmosphere perhaps the best natural laboratory for the study of ionized atoms. Atomic transitions at ultraviolet (UV) and X-ray wavelength regions generally show no optical depth effects, and the lines are not subject to the interstellar absorption that affects astronomical sources. Here I highlight the importance of atomic data to modeling UV and X-ray solar spectra, with a particular focus on the CHIANTI atomic database. Atomic data needs and problems are discussed and future solar mission concepts presented.

Keywords. Sun: UV radiation — Sun: X-rays, gamma rays — Sun: corona — atomic data

1. Introduction

The Sun is an ideal laboratory for studying magnetized plasmas on large spatial scales, as it can be studied through remote-sensing on time-scales of seconds at spatial resolutions down to 100 km over the complete electromagnetic spectrum. The macro-scale magnetic field is generated through complex plasma motions in the solar interior and evolves over the 11-year solar cycle. Above the solar surface, the magnetic field shapes the low density solar corona and is strongly implicated in heating the corona to over 1 million degrees, two orders of magnitude hotter than the 5800 K solar photosphere. Both the solar dynamo and coronal heating remain active areas of solar research, and more recently the impact of solar eruptive events on the Earth and human infrastructure has led to the new discipline of Space Weather.

At NASA, the major science questions in Solar Physics are defined as (1) how does the solar dynamo work; (2) how does the Sun's magnetism control its dynamic atmosphere; and (3) how is magnetic energy stored and explosively released. Progress on questions (2) and (3) critically depends on remote sensing of the solar atmosphere at soft X-ray, extreme ultraviolet (EUV) and far ultraiolet (FUV) wavelengths from 50 to 1600Å, which can only be done from space. Figure 1 shows a synthetic spectrum created with the CHIANTI database (described in the following section). There is a natural dividing line at 400Å, below which most of the lines are formed in the solar corona at temperatures of $\geqslant 1$ MK. Above the dividing line, most lines are formed in the solar transition region, a thin layer where the temperature rises abruptly by two orders of magnitude. Lines from the chromosphere at ≈ 10 kK appear above the hydrogen Lyman edge at 912 Å, and dominate the UV spectrum above 1600 Å.

The two main measurement techniques at these wavelengths are: (1) imaging spectroscopy, and (2) spectroscopic imaging. The former is classical spectroscopy: the Sun is imaged through a narrow slit that is dispersed on a grating to yield a 2D image of
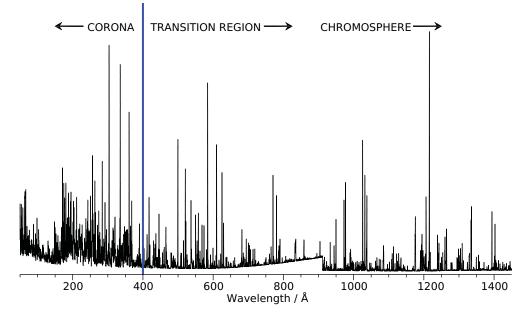
Figure 1. A simulated spectrum of the solar atmosphere from CHIANTI. The hydrogen Lyman edge is at 912 Å. The positions of emission features from different layers of the solar atmosphere are indicated.

wavelength vs. position along the slit. The latter is an imaging technique whereby narrowband filters are used to pick out particular spectral features. Ideally the images will give a clean "temperature slice" through the corona, corresponding to the temperature of formation of the emitting species, but interpretation can be complicated by additional species that contribute to the image bandpass.

To interpret the data from either of these measurement options, we need atomic data for the following:

(*a*) elements from hydrogen to zinc;

(*b*) ions from neutral to fully-ionized (temperatures 6000 to $> 10^7$ K); and

(*c*) line and continuum emission.

For Solar Physics the main repository of these data is the CHIANTI atomic database.

2. CHIANTI

CHIANTI (Dere *et al.* 1997; Young *et al.* 2016) is firstly an assessed database of atomic data for ions, and secondly a package of software for computing radiative emisions (both IDL and Python versions are available). As described in Young *et al.* (2016), CHIANTI is highly cross-disciplinary with many users working in Astrophysics, and there are also applications to laboratory plasmas and Planetary Science. Major updates are peformed every 2–3 years, and the current release is version 9 (Dere *et al.* 2019).

For the most part CHIANTI uses the assumption that atomic processes that affect state populations within an ion occur on faster timescales than processes related to ionization and recombination, and so state balance equations can be solved separately from ion balance equations.

For the state balance equations, the key atomic data-sets are experimental energies, electron collision strengths and radiative decay rates. All data are for fine structure levels. Supplemental data-sets (not available for all ions) include proton excitation rates, autoionization rates, and level-resolved radiative recombination and direct ionization
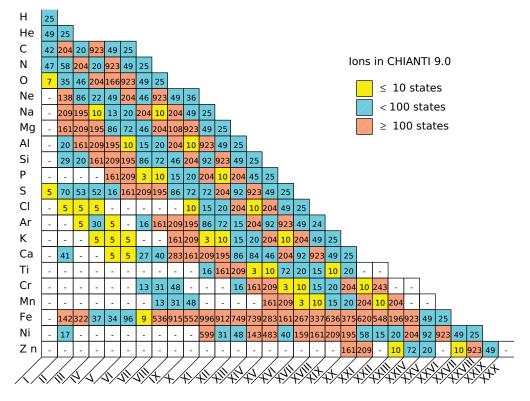
	I	II	III	IV	V	VI	VII	VIII	IX	X	XI	XII	XIII	XIV	XV	XVI	XVII	XVIII	XIX	XX	XXI	XXII	XXIII	XXIV	XXV	XXVI	XXVII	XXVIII	XXIX	XXX
H	25																													
He	49	25																												
C	42	204	20	923	49	25																								
N	47	58	204	20	923	49	25																							
O	7	35	46	204	166	923	49	25																						
Ne	-	138	86	22	49	204	46	923	49	36																				
Na	-	209	195	10	13	20	204	10	204	49	25																			
Mg	-	161	209	195	86	72	46	204	108	923	49	25																		
Al	-	20	161	209	195	10	15	20	204	10	923	49	25																	
Si	-	29	20	161	209	195	86	72	46	204	92	923	49	25																
P	-	-	-	-	161	209	3	10	15	20	204	10	204	45	25															
S	5	70	53	52	16	161	209	195	86	72	72	204	92	923	49	25														
Cl	-	5	5	5	-	-	-	-	-	10	15	20	204	10	204	49	25													
Ar	-	-	5	30	5	-	16	161	209	195	86	72	15	204	92	923	49	24												
K	-	-	-	5	5	5	-	-	161	209	3	10	15	20	204	10	204	49	25											
Ca	-	41	-	-	5	5	27	40	283	161	209	195	86	84	46	204	92	923	49	25										
Ti	-	-	-	-	-	-	-	-	-	-	16	161	209	3	10	72	20	15	10	20	-	-								
Cr	-	-	-	-	-	-	13	31	48	-	-	-	16	161	209	3	10	15	20	204	10	243	-	-						
Mn	-	-	-	-	-	-	13	31	48	-	-	-	-	-	161	209	3	10	15	20	204	10	204	-	-					
Fe	-	142	322	37	34	96	9	536	915	552	996	912	749	739	283	161	267	337	636	375	620	548	196	923	49	25				
Ni	-	17	-	-	-	-	-	-	-	-	599	31	48	143	483	40	159	161	209	195	58	15	20	204	92	923	49	25		
Zn	-	-	-	-	-	-	-	-	-	-	-	-	-	-	-	-	-	-	-	161	209	-	10	72	20	-	10	923	49	-

Ions in CHIANTI 9.0

- ≤ 10 states
- < 100 states
- ≥ 100 states

Figure 2. A summary of the ions contained in the CHIANTI database. The numbers in each box give the sizes of the atomic models.

rates. The ion coverage of CHIANTI for version 9 is shown in Figure 2, with the number of fine-structure states in the CHIANTI models indicated. We highlight the large models for the Li, B, F, Ne and Na isoelectronic sequences that come from the UK Atomic Processes for Astrophysical Plasmas (APAP; http://www.apap-network.org/) network. The coronal iron ions (Fe VIII–XXIV) are critical for studies of the solar atmosphere, and the CHIANTI team members have focussed a large effort on providing detailed models for these ions. Note that empty boxes in the table are either because there has not been a need for those ions, or because no fine-structure atomic data are available (particularly for electron excitation).

Ion-to-ion radiative and dielectronic recombination rates and ionization rates are included for all ions, and an ionization equilibrium file computed from the rates is distributed with the database.

A key part of CHIANTI is that all atomic data are assessed prior to being added to the database. The electron collision strengths are a particular focus of attention, and a graphical assessment technique is applied to each individual transition, allowing irregularities to be identified. The CHIANTI team have also done a number of benchmark studies, comparing observed solar spectra with CHIANTI predictions, to determine the accuracy of the atomic data (e.g., Young et al. 1998; Young & Landi 2009; Del Zanna 2012). The assessments have been crucial to community acceptance of CHIANTI, and this is recognized by the fact that a number of plasma codes and databases directly ingest atomic data from CHIANTI. For example, ATOMDB (Smith et al. 2001), CLOUDY (Ferland et al. 2017), XSTAR (Bautista & Kallman 2001) and MOCASSIN (Ercolano et al. 2008).
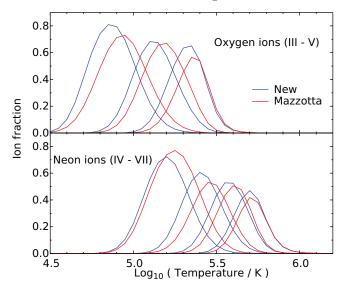
Figure 3. Ionization fraction curves for O III–V and Ne IV-VII from CHIANTI and Mazzotta *et al.* (1998), blue and red, respectively.

3. Data needs and problems

The distribution of ions as a function of temperature in equilibrium conditions is referred to as the ionization balance, and is determined principally by ionization and recombination rates between ions, summed over all states. The predicted emissivity of a given emission line directly depends on the ionization fraction and so uncertainties in the atomic rates can make a critical impact on derived physical parameters.

Ionization and recombination rates have seen significant updates in the past 15 years (Dere 2007; Badnell 2006; Badnell *et al.* 2003), which are reflected in changes to ionization fractions. Figure 3 compares ionization fractions for select ions of oxygen and neon between Mazzotta *et al.* (1998) and the latest compilation in CHIANTI. These ions were used by Young (2005) to determine the Ne/O relative abundance in the solar atmosphere. This ratio is important because it is not possible to measure the neon abundance in the solar photosphere, and so a proxy is necessary. In this case, ionized neon lines in the solar transition region ($T = 0.1$–0.3 MK) were used. Young (2018) updated the earlier results using the new ionization curves (Figure 3), and found a Ne/O ratio higher by 40%, mainly due to the updated ionization curves.

In general, so-called "zero-density" dielectronic recombination (DR) rates are used in astrophysics when computing the ionization balance, but it is known that DR rates can be suppressed at coronal densities of $\sim 10^{10}$ cm^{-3}. Density-sensitive rates are not generally available, but Nikolić *et al.* (2018) provided fitting formulae to unpublished data of Summers (1974), and Young *et al.* (2018) applied the derived rates to a study of density diagnostics in the solar atmosphere. They demonstrated significant decreases in the DR rates for many ions, even at relatively low densities. Figure 4 shows an example of how the ionization fraction of O VI increases and shifts to lower temperatures as the density increases.

Standard spectroscopic diagnostics of the solar atmosphere assume Maxwellian distributions for electrons and ions. During solar flares it is well-known that non-thermal electron distributions are produced as a consequence of magnetic reconnection occurring high in the corona. The electrons are braked when they hit the cool, dense chromosphere, giving rise to bremsstrahlung radiation that appears as a characteristic break in
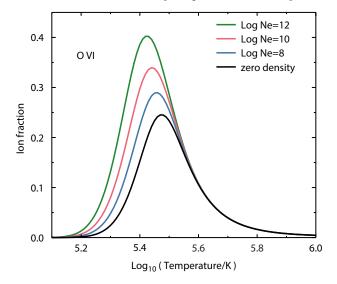
Figure 4. Ionization fractions as a function of density for O VI derived using the DR suppression formulae of Nikolić *et al.* (2018). The zero density case corresponds to the curve found in CHIANTI.
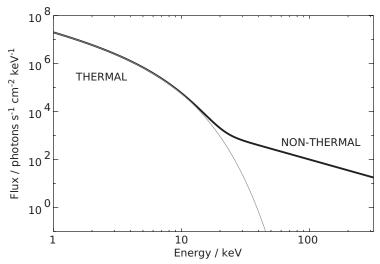

Figure 5. A simulated X-ray spectrum of a flare (black), with a power-law non-thermal component due to non-thermal electrons. The gray line shows emission due to thermal plasma (mostly free-free emission at 40 MK).

the X-ray spectrum above about 20 keV (Figure 5). In other solar structures evidence for non-thermal particle populations proved elusive, but recently Dudík *et al.* (2015) used EUV emission line ratios of Fe XI–XIII to identify electron kappa distributions in an observation of a coronal loop with the EUV Imaging Spectrometer (EIS) on board Hinode (Culhane *et al.* 2007). The kappa distribution function has an additional free parameter (κ) compared to Maxwellian distributions, such that the distribution tends to a Maxwellian for $\kappa \to \infty$. A key feature of the distribution is an enhanced high-energy tail compared to a Maxwellian, and it has been found to fit the electron distributions in the solar wind (Maksimovic *et al.* 1997). Evidence for kappa distributions for ions in the solar corona have been found during a solar flare by Jeffrey *et al.* (2016). The line profile

of Fe XVI 262.99 Å, again observed by EIS, was found to show small, but significant, deviations from a Gaussian shape that were consistent with a kappa distribution. Note that Dzifčáková *et al.* (2015) have adapted the atomic data in CHIANTI to create an atomic database that is based around kappa distributions rather than Maxwellian distributions.

Most of the strong lines in the 50–1600 Å range were identified in the 1960's and 70's through combinations of space and laboratory studies, but each new spectroscopy mission has led to new identifications. For example, Young (2009) identified four new lines of Fe IX observed by EIS in the 180–200 Å region. There continue to be many unidentified weak lines, however, and these are a particular problem for spectroscopic imaging instruments where such lines may impact the instrument response function. An example from the Atmospheric Imaging Assembly (AIA) instrument on board the Solar Dynamics Observatory was for the channel centered at 94 Å. This part of the spectrum has rarely been observed, and it was clear there was unexpected spectral "contamination" (Aschwanden & Boerner 2011). Del Zanna (2012) made a new Fe XIV identification from 1960's rocket spectra in this range that improved the CHIANTI models.

This example highlights the need for continued laboratory studies of X-ray and UV spectra. For example, Beiersdorfer & Träbert (2018) reported new identifications of lines contributing to the AIA 171 Å channel.

In general, plasma modeling codes such as CHIANTI do not provide estimates of uncertainties on either the atomic data, or the line emissivities. This is a problem as modern solar spectra often have high signal-to-noise, and thus when a least-squares fitting is performed, for example, to determine a differential emission measure, the resulting χ^2 values can be very large. It is then common to assign a uniform uncertainty of typically 15–20% to all emission lines that is understood to represent the atomic data uncertainties (e.g., Landi & Young 2009).

As discussed earlier, the key atomic data-sets for coronal emission line analysis are radiative decay rates and electron collision strengths, and the vast majority of data in CHIANTI comes from theoretical calculations. Due to the greater complexity of the calculations for collision strengths, these are expected to be the most uncertain. Typically atomic physicists assign an uncertainty that is a single percentage for all transitions. Comparisons of calculations using different codes or structure models provide a means for assessing uncertainties on a transition-by-transition basis, such as done for N IV (Del Zanna *et al.* 2019).

Efforts to propagate atomic data uncertainties into the plasma diagnostic uncertainties have recently been performed by Yu *et al.* (2018). They assigned uncertainties between 5 and 50% to the collision strengths of individual atomic transitions according to how well the collision strengths of Del Zanna & Storey (2012) agreed with the earlier calculation of Storey & Zeippen (2010). For the radiative decay rates, they sorted the calculated values of Del Zanna & Storey (2012) into groups based on value, assigning uncertainties of 5, 10 or 30% to the three groups. Propagating the atomic data certainties through the CHIANTI emissivity calculations, the authors were able to obtain density diagnostic line ratio plots with realistic uncertainties.

4. Future instrumentation

Solar Physics is mostly a mission-driven field: advances in spectral coverage, spatial resolution and temporal resolution reveal new phenomena or new insights into familiar events such as flares. The previous 25 years has been a golden age for the field, with continued improvement in observing capabilties from SOHO (launched in 1995) to SDO and IRIS (2010 and 2013). The next major solar mission is ESA's Solar Orbiter, scheduled to be launched in 2020 February, that will feature an EUV imaging spectrometer called

SPICE (Anderson *et al.* 2019) and an EUV spectroscopic imager called EUI (Halain *et al.* 2015). The most advanced ground-based solar telescope, DKIST, will become operational in 2020 and, although unable to access the X-ray and UV regions discussed in the present work, it will measure a number of coronal forbidden lines above the solar limb that will complement the X-ray and UV studies (e.g., Snow *et al.* 2018).

Two new EUV spectroscopy mission concepts have been proposed to NASA. The Multi Slit Solar Explorer (MUSE; Cheung *et al.* 2019a) was selected for a Phase A Small Explorer satellite study in 2017, but unfortunately was not selected for Phase B in 2019. It took the novel approach of observing the Sun through 37 parallel slits, thus enabling simultaneous 2D imaging and high-resolution spectroscopy in three narrow wavebands (Cheung *et al.* 2019b). Solar-C_EUVST is a Japanese mission concept with US support, that was proposed to both JAXA and NASA in 2018. It is an imaging spectrometer, the unique feature being seamless coverage of all layers of the solar atmosphere through simultaneous coverage of four wavelength bands between 170 and 1250 Å. Solar-C_EUVST is based on the LEMUR concept described in Teriaca *et al.* (2012).

References

Anderson, M., Appourchaux, T., Auchère, F., *et al.* 2019, arXiv e-prints, arXiv:1909.01183
Aschwanden, M. J. & Boerner, P. 2011, *ApJ*, 732, 81
Badnell, N. R. 2006, *ApJS*, 167, 334
Badnell, N. R., O'Mullane, M. G., Summers, H. P., *et al.* 2003, *A&A*, 406, 1151
Bautista, M. A. & Kallman, T. R. 2001, *ApJS*, 134, 139
Beiersdorfer, P. & Träbert, E. 2018, *ApJ*, 854, 114
Cheung, M. C. M., De Pontieu, B., Martínez-Sykora, J., *et al.* 2019a, *ApJ*, 882, 13
Cheung, M. C. M., De Pontieu, B., Martınez-Sykora, J., *et al.* 2019b, *ApJ*, 882, 13
Culhane, J. L., Harra, L. K., James, A. M., *et al.* 2007, *Sol. Phys.*, 243, 19
Del Zanna, G. 2012, *A&A*, 546, A97
Del Zanna, G., Fernández-Menchero, L., & Badnell, N. R. 2019, *MNRAS*, 484, 4754
Del Zanna, G. & Storey, P. J. 2012, *A&A*, 543, A144
Dere, K. P. 2007, *A&A*, 466, 771
Dere, K. P., Del Zanna, G., Young, P. R., Landi, E., & Sutherland, R. S. 2019, *ApJS*, 241, 22
Dere, K. P., Landi, E., Mason, H. E., Monsignori Fossi, B. C., & Young, P. R. 1997, *A&AS*, 125, 149
Dudík, J., Mackovjak, Š., Dzifčáková, E., *et al.* 2015, *ApJ*, 807, 123
Dzifčáková, E., Dudík, J., Kotrč, P., Fárník, F., & Zemanová, A. 2015, *ApJS*, 217, 14
Ercolano, B., Young, P. R., Drake, J. J., & Raymond, J. C. 2008, *ApJS*, 175, 534
Ferland, G. J., Chatzikos, M., Guzmán, F., *et al.* 2017, *Rev. Mexicana Astron. Astrofis.*, 53, 385
Halain, J.-P., Mazzoli, A., Meining, S., *et al.* 2015, in *Proc. SPIE*, Vol. 9604, Solar Physics and Space Weather Instrumentation VI, 96040H
Jeffrey, N. L. S., Fletcher, L., & Labrosse, N. 2016, *A&A*, 590, A99
Landi, E. & Young, P. R. 2009, *ApJ*, 706, 1
Maksimovic, M., Pierrard, V., & Riley, P. 1997, *Geophys. Res. Lett.*, 24, 1151
Mazzotta, P., Mazzitelli, G., Colafrancesco, S., & Vittorio, N. 1998, *A&AS*, 133, 403
Nikolić, D., Gorczyca, T. W., Korista, K. T., *et al.* 2018, *ApJS*, 237, 41
Smith, R. K., Brickhouse, N. S., Liedahl, D. A., & Raymond, J. C. 2001, *ApJ*, 556, L91
Snow, B., Botha, G. J. J., Scullion, E., *et al.* 2018, *ApJ*, 863, 172
Storey, P. J. & Zeippen, C. J. 2010, *A&A*, 511, A78
Summers, H. P. 1974, *MNRAS*, 169, 663
Teriaca, L., Andretta, V., Auchère, F., *et al.* 2012, *Experimental Astronomy*, 34, 273
Young, P. R. 2005, *A&A*, 439, 361
—. 2009, *ApJ*, 691, L77
—. 2018, *ApJ*, 855, 15

Young, P. R., Dere, K. P., Landi, E., Del Zanna, G., & Mason, H. E. 2016, *J. Phys. B: At. Mol. Phys.*, 49, 074009

Young, P. R., Keenan, F. P., Milligan, R. O., & Peter, H. 2018, *ApJ*, 857, 5

Young, P. R. & Landi, E. 2009, *ApJ*, 707, 173

Young, P. R., Landi, E., & Thomas, R. J. 1998, *A&A*, 329, 291

Yu, X., Del Zanna, G., Stenning, D. C., *et al.* 2018, *ApJ*, 866, 146